Simulation of photophysical processes of indoles in solution

John D. Westbrook, Ronald M. Levy, and Karsten Krogh-Jespersen

Rutgers University, Department of Chemistry
New Brunswick, New Jersey 08903

ABSTRACT

Computational studies of photophysical processes in solution require accurate representations of the potential energy function. The interactions in a polar solute-solvent system are primarily electrostatic in nature and they are in molecular simulations typically mediated by partial atomic charges on the solute and the solvent atoms. We have developed procedures to create partial atomic charges for any electronic state in a solute molecule from a least squares fit to the molecular electrostatic potential. The quantum mechanical electrostatic potential for the electronically excited ^1L_a state of 3-methylindole derived from a semiempirical INDO/S configuration interaction wavefunction is presented. Partial atomic charges for the ^1L_a state are derived from the quantum mechanical potential and the classical and quantum mechanical electrostatic potentials are compared. Molecular dynamics simulations have been carried out on the ground (S_0) and two lowest excited singlet states (^1L_b, ^1L_a) of 3-methylindole in water using potential derived partial atomic charges. Solvent induced inversion of the gas phase excited state ordering (^1L_b below ^1L_a) is computed for the excited states. A method for introducing polarization by the solvent into the solute electronic wavefunctions and hence into the solute partial atomic charges is introduced. A significant increase in solute dipole moment is computed for the ^1L_a state, leading to dramatic increases in solute-solvent interaction energies and additional preferential stabilization of the ^1L_a state over the ^1L_b state.

1. INTRODUCTION

Simulations of molecular photophysical processes in solution is a demanding but highly important problem for computational chemists to address. A large number of intermolecular interactions must be considered to correctly reflect the intricate physics of the solute-solvent system. Thus, accurate physical models must be developed with implementations that are computationally tractable and applicable to a wide variety of problems. We are presently involved in formulating such computational models, their implementation, and their application to systems of biological relevance.[1-7] Principal components of our methodology include the extensive use of both quantum mechanical electronic structure techniques and molecular dynamics simulation methods based on classical and statistical mechanics principles. Our models are distinctly microscopic in nature and sufficiently detailed to provide insight into a variety of photophysical processes including the structural origins of solvent-induced line shifts and broadening in optical absorption and time-resolved fluorescence spectra of a solvated molecule.[2,4]

For polar solutes in polar media, the dominant intermolecular interactions are electrostatic in nature. The interactions are typically modeled with partial atomic charges acting as monopoles at the nuclear positions and when both solute and solvent molecules are treated in a fully classical framework, the electrostatic solute-solvent term becomes just a simple sum over pairwise coulombic interaction energies. An alternative approach to the study of electrostatic solute-solvent interactions, applicable when the solute is treated in a quantum mechanical framework via electronic structure theory, is to incorporate the coulombic effect of the solvent into the molecular Hamiltonian as an additional one-electron operator, thus allowing the solute electronic structure to adjust to the presence of the solvent. The solute atomic charges used in molecular dynamics simulations are most often kept fixed during the simulations and derived from electronic structure wavefunctions calculated for an isolated molecule. They are

 0-8194-0786-0/92/$4.00

Downloaded from SPIE Digital Library on 21 Oct 2009 to 128.6.69.52. Terms of Use: http://spiedl.org/terms

consequently appropriate to an idealized vacuum situation. However, the partial atomic charges ought to represent the solute in the presence of the solvent, potentially a major difference if the solute electronic structure undergoes a significant change through polarization by the solvent. Furthermore, the altered electrostatic properties of the polarized solute should be transmitted back to the solvent and the polarization process repeated until self-consistency has been reached.

The electronic states of indoles provide an excellent vehicle for the study of polar solute-solvent interactions. Indole is the chromophore for the amino acid tryptophane, the dominant naturally occurring fluorophore in proteins,[8] and its basic spectroscopic properties have been studied extensively.[9,10] Two close-lying electronically excited singlet states in the near UV region, denoted ^1L_b and ^1L_a, are of fundamental importance. The indole ^1L_a state has a much larger dipole moment (~5 D)[11] than the ground state (2.1 D)[12] or the ^1L_b state (~2.3 D)[13] and is observed in the gas phase at slightly higher energy than the ^1L_b state.[9] However, due to the significant differences in dipole moments the state ordering is readily reversed in polar solvent. The actual ^1L_a-^1L_b energy separation and many other excited state features of indoles show strong dependence on the solvent polarity,[14] and the general photophysical properties of indoles thus reflect the detailed natures of both the chromophore and the surrounding medium. The magnitude of the tryptophane fluorescence Stokes shift, for example, provides a spectroscopic marker of the polarity exerted by the environment of a particular tryptophane residue in a protein.[15]

We have carried out a number of electronic structure calculations and molecular dynamics simulations on 3-methylindole (3-MeIn) in water to investigate the electrostatic interactions in the electronic ground (S_0) and lower excited singlet states (^1L_b, ^1L_a). We discuss here briefly our method for obtaining the molecular electrostatic potential and partial atomic charges. We apply potential derived charges in a series of simulations to investigate the solvent effects on the electronic states of 3-MeIn and outline a scheme for introducing polarization effects into the simulations. Electronic polarization of the solute by the solvent is found to be substantial and leads to large increases in the electrostatic interaction energies.

2. METHODOLOGY

The electronic structure calculations have been carried out with the ESPPAC program,[16] a molecular orbital package based on the semiempirical, all valence-electron INDO model Hamiltonian specifically designed and parameterized for calculations of properties associated with electronically excited states (INDO/S).[17] Configuration interaction calculations utilizing all single excitations (600) were carried out to obtain the wavefunctions for the ground and lowest excited states of 3-MeIn. A number of properties, including the electronic transition energies, state and transition dipole moments, and molecular electrostatic potentials were computed from the wavefunctions.

All molecular dynamics calculations were performed with the IMPACT program package[18] at constant temperature and pressure (298 K and 1 atm) with periodic boundary conditions. The simulations included one 3-MeIn solute molecule and 394 SPC water molecules.[19] The coulombic interactions were modeled simply as

$$E_{int}(\text{solute-solvent}) = \Sigma\, Q_S Q_A / |R_S - R_A| \qquad (1)$$

where Q_S and Q_A represent the partial atomic charges on the solvent (SPC model) and solute atoms, respectively, and $|R_S - R_A|$ is the distance between a solvent and a solute atom. The solute partial atomic charges were derived from fits to the quantum mechanical electrostatic potential (see below) appropriate to the S_0, ^1L_b, or ^1L_a electronic states of 3-MeIn. Simulations were run for approximately 10 ps using an integration time step of 2 fs. The electrostatic contributions to the differential solvation energies (ΔG) were evaluated with a recently proposed dielectric function based on linear response theory [6,20]

Downloaded from SPIE Digital Library on 21 Oct 2009 to 128.6.69.52. Terms of Use: http://spiedl.org/terms

$$\Delta G = \Sigma \langle V_i \rangle \Delta Q_i - 0.5 * \beta \Sigma \langle \Delta V_i \Delta V_j \rangle \Delta Q_i \Delta Q_j \quad (2)$$

In this formula, $\Delta Q_i = Qg_i - Qe_i$ denoted the difference in partial atomic charge at the i'th atom of the solute in the ground(Qg_i) and excited (Qe_i) states and $\beta = 1/k_BT$. The formula also contains the average electrostatic potential from the solvent at the atomic centers of the solute, $\langle V_i \rangle$, as well as the correlation functions for the joint fluctuations in the solvent electrostatic potential at solute sites i and j, $\langle \Delta V_i \Delta V_j \rangle$. The averages were extracted from a long reference simulation on the ground state of 3-MeIn in water (100 ps).[6]

An interface between the two computer programs (ESPPAC and IMPACT) facilitated mixed mode calculations in which the solute was treated quantum mechanically with the coulombic effects from the solvent explicitly included in the solute electronic Hamiltonian.[21] That is,

$$H_{el} = H_{el}(\text{INDO/S}) + H_{int}(\text{solute-solvent}) = H_{el}(\text{INDO/S}) + \Sigma Q_S Q_e / |R_S - r| \quad (3)$$

where Q_S again represents the partial atomic charges on the solvent atoms, Q_e is the electronic charge, and $|R_S - r|$ is the distance between a solvent atom and an electron in the solute. The interaction operator will modify the electronic wavefunction of the solute relative to its vacuum appearance (determined by H_{el}(INDO/S) alone) and hence change the electronic properties of the solvated molecule.

3. ELECTROSTATIC POTENTIAL DERIVED PARTIAL ATOMIC CHARGES

We have recently presented a general set of procedures for deriving partial atomic charges from the molecular electrostatic potential, applicable to any (ground or excited) electronic state. The underlying wavefunctions may be computed from an independent particle model (Hartree-Fock) or with correlation corrections included (configuration interaction, perturbation theory), and they can be ab initio or semiempirical in nature.[7]

The molecular electrostatic potential in a spatial point r is defined as[22]

$$V(r) = \Sigma Z_A / |R_A - r| - \int \rho(r') / |r' - r| \, dr' = \Sigma Z_A / |R_A - r| - \Sigma p_{\mu\nu} \int \phi_\mu(r') \phi_\nu(r') / |r' - r| \, dr' \quad (4)$$

where Z_A is the core charge of nucleus A at position R_A, $\rho(r')$ is the electron density at the point r', and $p_{\mu\nu}$ is the element of the one-electron reduced density matrix between the atomic basis functions ϕ_μ and ϕ_ν.[23] A set of partial atomic charges (Q_A) may be obtained from a linear, least squares fit of the classical electrostatic potential exerted by such charges ($E(r, Q_A) = \Sigma Q_A / |R_A - r|$) to the quantum mechanical electrostatic potential (V(r)) sampled over a number of points at the molecular van der Waals surface and beyond, the region where intermolecular interactions occur.[24] Our particular sampling procedure and its merits are discussed in reference 7. Potential derived atomic charges for ground or electronically excited states should be superior in molecular dynamics simulations to atomic charges provided by traditional wavefunction population analyses (ZDO or Mulliken), since the fitted charges automatically reproduce the quantum mechanical dipole moment well, thus assuring that long range electrostatic interactions of the dipole-dipole type will be represented correctly.

We show below in Figure 1 the quantum mechanical molecular electrostatic potential for the ^1L_a state of 3-MeIn in the molecular plane based on an INDO/S wavefunction including all singly excited configurations. The reduced density matrix ($p_{\mu\nu}$) is computed using deorthogonalized atomic orbitals[25] represented by STO-6G expansions[26] and V(r) is evaluated according to equation (4). The hydrogen

Downloaded from SPIE Digital Library on 21 Oct 2009 to 128.6.69.52. Terms of Use: http://spiedl.org/terms

atoms dominate the in-plane potential near the molecule and solid contours of positive electrostatic potential (repulsive to a positive test charge) envelop the entire molecule. The potential is decidedly repulsive in wide regions around the pyrrole ring but becomes attractive at distances of about 1 A and beyond from the hydrogen atoms on the benzene ring. These regions correspond to the positive and negative ends of the molecular dipole, respectively.

The molecular electrostatic potential is sampled at a number of points (~6,000) and a set of classical charges are obtained using a Lagrange multiplier based linear, least-squares fit of the function

$$Y(Q_A) = \Sigma(V(r) - E(r, Q_A))^2 \quad (5)$$

expressing the squares deviation between the quantum mechanical and classical electrostatic potentials over the sampled points, subject to the constraint that ΣQ_A = total molecular charge. The derived partial atomic charges and the direction and magnitude of the dipole moment for the ^1L_a state are shown in Figure 2.[27] The classical potential $E(r, Q_A)$ exerted by these charges in the molecular plane is shown in Figure 3. The classical electrostatic potential shows a nodal surface between any two neighboring atoms containing charges of opposite sign whereas the quantum mechanical potential does not. Thus, the molecular electrostatic potential can not be approximated by monopoles in the immediate vicinity of the molecule but in the range of distances where intermolecular contacts occur, Figures 1 and 3 are qualitatively similar. Figure 4 shows the difference between the quantum mechanical (V(r), Figure 1) and classical ($E(r, Q_A)$, Figure 2) electrostatic potentials at and outside the Van der Waals surface and gives an indication of the overall quality of the fit. Contour value comparisons show that the monopoles approximate the quantum mechanical potential very well at long distances whereas closer up to the molecule (near the van der Waals surface) the fit is poorer and deviations larger than 10% may be noted near the innermost point sampling surface. Partial atomic charges were also derived for the ground state (S_0) and the ^1L_b excited state of 3-MeIn for use in the molecular dynamics simulations described next.[7]

4. MOLECULAR DYNAMICS SIMULATIONS; ^1L_a-^1L_b ENERGY DIFFERENCE

The energy separation between the indole ^1L_b and ^1L_a states in the gas phase is estimated near 1,400 cm^{-1} with the ^1L_b state lower in energy; the origin of the ^1L_b state appears as a broad feature near 35,200 cm^{-1}.[9] The Franck-Condon maximum for the ^1L_b state nearly coincides with the origin whereas the absorption maximum for the ^1L_a state is estimated nearly 3,000 cm^{-1} higher around 38,000 cm^{-1}.[10,28] The spectra of 3-MeIn are not as well analyzed. The ^1L_b origin in the gas phase is at 34,800 cm-1 and the origin of the ^1L_a state is at least 100 cm^{-1} higher in energy but it has not been clearly identified.[9] The difference in Franck-Condon maxima between the two states in 3-MeIn is near 2,200 cm^{-1}.[10] An INDO/S electronic structure calculation on 3-MeIn (geometry optimized at the ab initio Hartree-Fock level with a 6-31G* basis set) including all the singly excited configurations predicts the vertical transition to the ^1L_b state at 33,900 cm^{-1} and that to the ^1L_a state at 35,500 cm^{-1}, for a computed difference of 1,600 cm^{-1} in very good agreement with the available experimental data. The computed dipole moments for the three states in question are S_0 (1.8 D), ^1L_b (2.9 D), and ^1L_a (4.3 D), also in good agreement with the available experimental values (for the parent indole).

Molecular dynamics simulations using the potential derived charges for the ground state (S_0) and the excited ^1L_a state predict a differential solvation energy (equation 2) between the two states of 3.3 kcal/mol in favor of ^1L_a, the electronic state with the larger dipole moment. Simulating with the S_0 and ^1L_b charges leads to a preferential stabilization of the ^1L_b state by only 0.8 kcal/mol, in qualitative accordance with the small difference in dipole moments between these two states. Thus, the computed level separation in vacuum is 1,600 cm^{-1} with the ^1L_b state lowest, but the computed preferential stabilization arising solely from the altered charged distributions interacting with the polar water solvent

Downloaded from SPIE Digital Library on 21 Oct 2009 to 128.6.69.52. Terms of Use: http://spiedl.org/terms

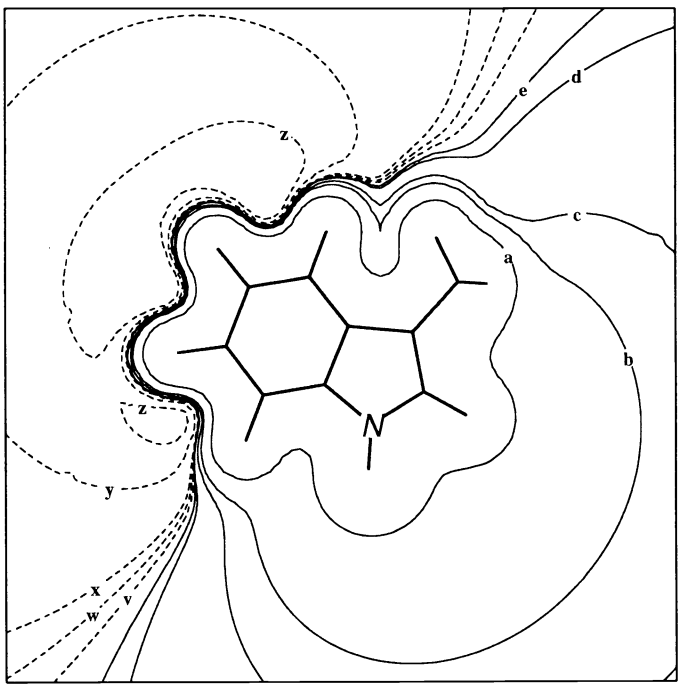

Figure 1. The quantum mechanical molecular electrostatic potential for the ^1L_a state of 3-methylindole computed from an INDO/S configuration interaction wavefunction and plotted in the molecular plane. The contour levels (in Hartrees; 1 Hartree = 627.5 kcal/mole) are as follows: a = 0.05; b = 0.01; c = 0.005; d = 0.001; e = 0.0005; and z = -0.01; y = -0.005; x = -0.001; w = -0.0005 and v = -0.00001.

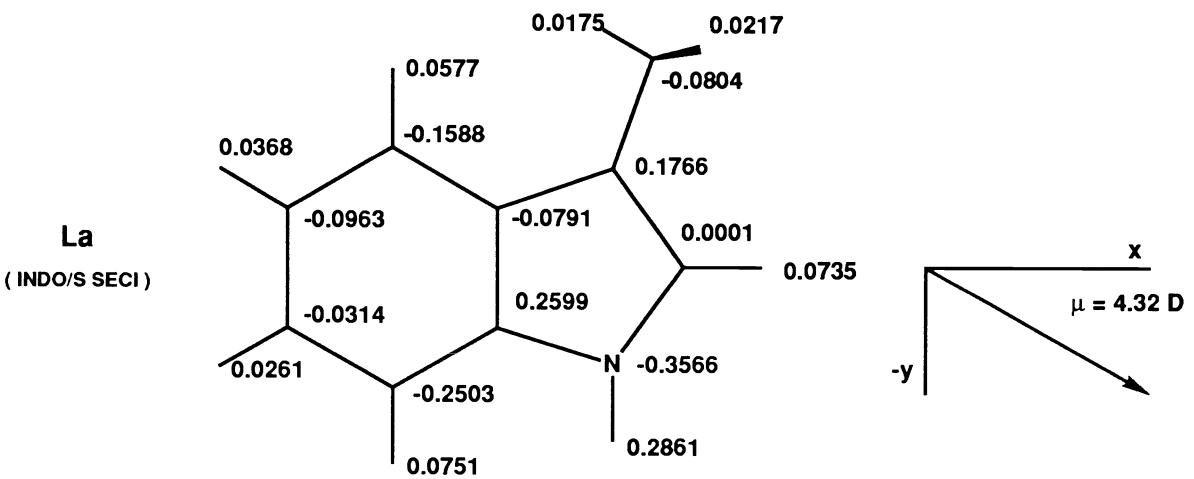

Figure 2. Partial atomic charges for the ^1L_a excited state of 3-methylindole obtained from a fit to the quantum mechanical molecular electrostatic potential shown in Figure 1. The dipole moment magnitude and direction is also shown.

Downloaded from SPIE Digital Library on 21 Oct 2009 to 128.6.69.52. Terms of Use: http://spiedl.org/terms

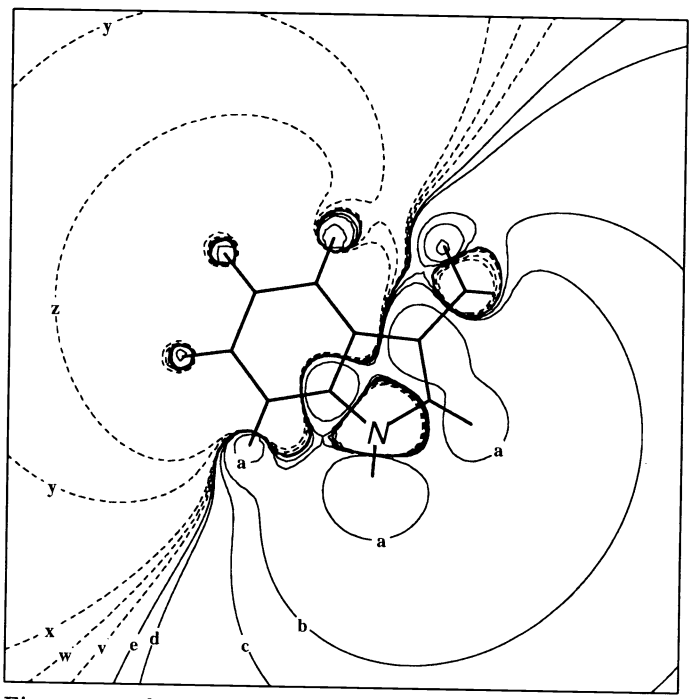

Figure 3. The classical electrostatic potential exerted by the fitted charges for the ^1L_a excited state shown in Figure 2, plotted in the molecular plane. The contour levels are the same as those used in Figure 1.

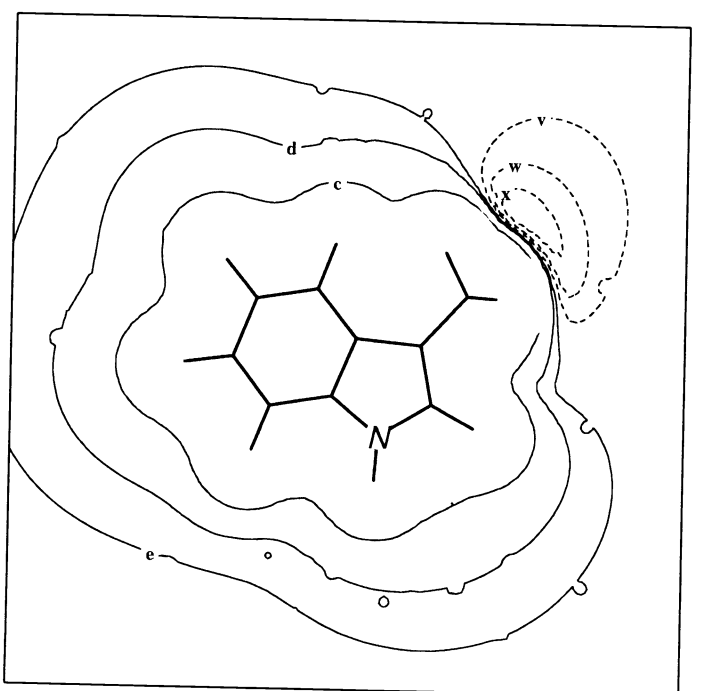

Figure 4. The difference between the quantum mechanical and classical electrostatic potentials (Figures 1 and 3, respectively) plotted in the molecular plane. The contour levels are the same as those used in Figure 1.

Downloaded from SPIE Digital Library on 21 Oct 2009 to 128.6.69.52. Terms of Use: http://spiedl.org/terms

is 2.5 kcal/mol (875 cm^{-1}) in favor of ^1L_a. Combining the two sets of data (electronic structure, molecular dynamics) we obtain an ^1L_a-^1L_b state energy difference of only ~ 700 cm^{-1} but no excited state level inversion.

Although the ^1L_a state is computed from our simulations to be the more highly solvated state in water, the computed stabilization energy appears far too small. The reported values for the solvent shift ($\Delta\nu_{max}$(absorption) - $\Delta\nu_{max}$(fluorescence)) of indole in polar solvents relative to hexane are ~5 kcal/mol (e.g. 4.6 kcal/mol in acetonitrile; 5.7 kcal/mol in ethanol) and the shifts for 3-methylindole in polar solvents relative to cyclohexane are even larger (8.5 kcal/mol in acetonitrile; 9.1 kcal/mol in butanol).[11] The solvent shift of indole in water (relative to hexane) appears to be anomalously high, about 12 kcal/mol, and that of 3-MeIn in water (relative to cyclohexane) is even larger and near 17 kcal/mol.[11] These large solvation energies have been attributed to the presence of specific solvent-solute interactions such as exciplex formation.[29] It should be noted that a previous combined electronic structure/molecular dynamics study obtained an even smaller solvation stabilization energy for the ^1L_a state and no level inversion.[28] The experimentally measured shifts are also quite different from those predicted by the simple Onsager dipole cavity reaction field formula[30]

$$\Delta G = 2 * (\Delta\mu)^2 f(\varepsilon)/ a^3 \qquad (6)$$

Here ΔG is the solvent reorganization free energy, $\Delta\mu$ is the change in dipole moment between the ground and the excited state, a is the radius for the spherical cavity, and $f(\varepsilon) = (\varepsilon-1)/ (2\varepsilon + 1)$ is a dielectric function (ε = solvent static dielectric constant). Application of this formula with a = 3.4 A,[11] ε = 81, and the computed dipole moments predicts that the ^1L_b - S_0 solvation energy difference should be ~ 0.5 kcal/mol and the ^1L_a - S_0 difference ~ 2.3 kcal/mol. We have previously discussed the inability of the Onsager formula to properly predict the solvent reorganization energy for spatially extended systems.[6]

One major reason for the discrepancy between observed and computed solvent shifts could be that the computations omit the electronic polarization of the solute by the solvent.[31] Our results for a model dipolar system (formaldehyde in water) suggest that this effect will lead to more polar solute states.[2] Since the ^1L_a state inherently has the larger dipole moment, it seems likely that inclusion of polarization in the simulations will increase the computed ^1L_a-^1L_b separation. To investigate this further we employ the following scheme: (a) molecular dynamics simulations are initiated with the (gas phase) charges for the appropriate electronic state (S_0, ^1L_b, or ^1L_a) as described above; (b) after 50 time steps (100 fs), the entire solute-solvent configuration is selected for an electronic structure calculation using the INDO/S Hamiltonian; (c) the quantum mechanical electrostatic potential is computed from the configuration interaction wavefunction created for the solute, and a new set of potential derived partial atomic charges is derived. These charges now include polarization in the solute by the solvent; (d) the new set of charges are fed back into the molecular dynamics simulations, after another 50 time steps a new solute-solvent configuration is selected for a full electronic structure calculation, the electrostatic potential and charges are computed, etc.. These procedures continue until some satisfactory level of self-consistency has been reached.

In Figures 5 and 6 we show the effects of polarization on the dipole moments and the electrostatic solvation energies for S_0 (Figure 5) and ^1L_a (Figure 6) in 3-MeIn. The initial (gas phase) dipole moments of 1.8 D (S_0) and 4.3 D (^1L_a) increase very rapidly to reach their average limiting values of about 2.4 D (S_0) and 10.3 D (^1L_a). The dipole moment for the ^1L_b state (not shown) similarly increases from 2.9 D to 5.3 D with the inclusion of polarization. As anticipated, the dipole moment

Downloaded from SPIE Digital Library on 21 Oct 2009 to 128.6.69.52. Terms of Use: http://spiedl.org/terms

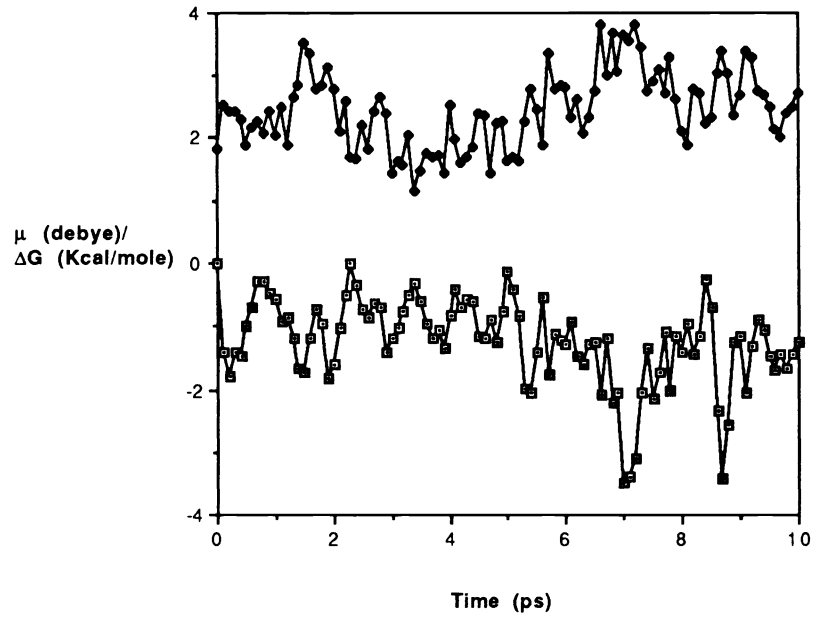

Figure 5. The time evolution of the dipole moment and electrostatic solvation energy for the ground state (S_0) of 3-methylindole using the self-consistent polarization scheme described in the text. The reference state for the solvation energy is the unpolarized ground state.

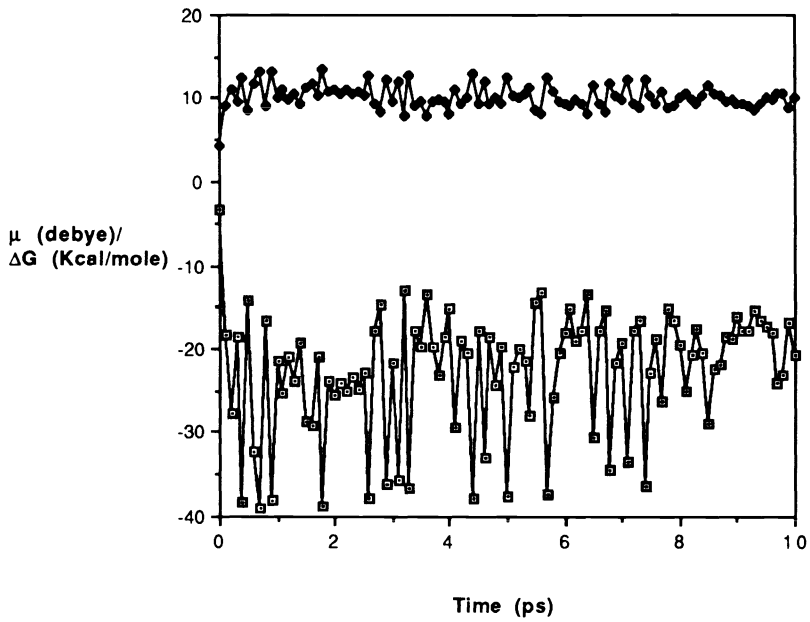

Figure 6. The time evolution of the dipole moment and electrostatic solvation energy for the ^1L_a excited state of 3-methylindole using the self-consistent polarization scheme in the text. The reference state for the solvation energy is the unpolarized ground state. Notice the difference in vertical scales between Figures 5 and 6.

Downloaded from SPIE Digital Library on 21 Oct 2009 to 128.6.69.52. Terms of Use: http://spiedl.org/terms

increase in the ^1L_a state is thus much larger (6.0 D) than the increases computed for the ^1L_b (2.4 D) and S_0 (0.6 D) states but even the latter changes are far from negligible.

These substantial changes in solute dipole moments in turn lead to dramatically increased differential solvation energies for the more polar electronically excited states. The polarized charges predict an electrostatic stabilization of S_0 relative to the unpolarized S_0 of only 1.2 kcal/mol (Figure 5), in accordance with the small increase in dipole moment. However, the polarized ^1L_b and ^1L_a states are preferentially stabilized relative to the polarized S_0 state by 4.3 (not shown) and 21.4 kcal/mol (Figure 6), respectively, substantially larger relative solvation energies than those obtained with the unpolarized charges (see above). Combining these differential solvation energy values with the computed value for the gas phase ^1L_b-^1L_a separation (1,400 cm^{-1}) we do predict excited state level inversion, since the hydrated ^1L_a state now lies 13.1 kcal/mol (4,600 cm^{-1}) below the hydrated ^1L_b state.

5. CONCLUDING REMARKS

We have investigated the electrostatic interactions between three different electronic states in 3-methylindole and water. The partial atomic charges for the particular electronic state of the solute under investigation were obtained from fits to the quantum mechanical molecular electrostatic potential. A self-consistent scheme for introducing electronic polarization into such charges was presented and found to lead to dramatic increases in solute dipole moments and solute-solvent electrostatic interaction energies. The anticipated ^1L_b-^1L_a level inversion was only obtained when the polarized charges were used in the simulations. Whereas the computed solvent shift for the ^1L_a state is much too small with the unpolarized charges (3.3 kcal/mol), the predicted solvent shift based solely on the electrostatic energies with the polarized charges (21.4 kcal/mol) is in qualitative agreement with, and even slightly than larger than, the value inferred from the experimental data (~ 17 kcal/mol). It is likely that the highly polarized ^1L_a state has pulled the solvating water molecules in very tightly and that an increase in nonbonded (Lennard-Jones) interactions has occurred relative to the situation created by the unpolarized charges. This would diminish the overall change in the total solvation energy and hence decrease the computed solvent shift. We are presently investigating this and other issues related to solvation of polar molecules in polar solvents through additional analysis and simulations of 3-methylindole and the tryptophane zwitterion in water.

6. ACKNOWLEDGMENTS

Financial support for this work was provided by the National Science Foundation (DMB 91-05208), a Biomedical Research Support Grant (PHS RR 07058-25), and a grant from the David and Johanna Busch Memorial Fund. Generous grants of supercomputer time at the National Cancer Institute Supercomputer Facility of the National Institute of Health and the Pittsburgh Supercomputer Center are gratefully acknowledged.

7. REFERENCES

1. J. T. Blair, J. D. Westbrook, R. M. Levy, and K. Krogh-Jespersen, *Chem. Phys. Lett.*, 154, 531, 1989.
2. J. T. Blair, K. Krogh-Jespersen, and R. M. Levy, *J. Am. Chem. Soc.*, 111, 6948, 1989.
3. J. T. Blair, R. M. Levy, and K. Krogh-Jespersen, *Chem. Phys. Lett.*, 166, 429, 1990.
4. R. M. Levy, D. B. Kitchen, J. T. Blair, and K. Krogh-Jespersen, *J. Phys. Chem.*, 94, 4470, 1990.
5. M. Belhadj, D. B. Kitchen, K. Krogh-Jespersen, and R. M. Levy, *J. Phys. Chem.*, 95, 1082, 1991.
6. R. M. Levy, J. D. Westbrook, D. B. Kitchen, and K. Krogh-Jespersen, *J. Phys. Chem.*, 95, 6756, 1991.

Downloaded from SPIE Digital Library on 21 Oct 2009 to 128.6.69.52. Terms of Use: http://spiedl.org/terms

7. J. D. Westbrook, R. M. Levy, and K. Krogh-Jespersen, "Molecular Electrostatic Potentials and Partial Atomic Charges From Correlated Wavefunctions: Application to the Electronic Ground and Excited States of 3-Methylindole," submitted to J. Comp. Chem. for publication.
8. J. R. Beecham and L. Brand, *Annu. Rev. Biochem.*, 54, 43, 1985.
9. J. R. Cable, *J. Chem. Phys.*, 92, 1627, 1990.
10. P. R. Callis, *J. Chem. Phys.*, 95, 4230, 1991.
11. H. Lami and N. Glasser, *J. Chem. Phys.*, 84, 597, 1986. S. R. Meech, D. Phillips, and A. G. Lee, *Chem. Phys.*, 80, 317, 1983. M. Sun and P. S. Song, *Photochem. Photobiol.*, 25, 3, 1977.
12. A. L. McClellan, Tables of Experimental Dipole Moments, Freeman, London, 1963.
13. C.-T. Chang, C.-Y. Wu, A. R. Muirhead, and J. R. Lombardi, *Photochem. Photobiol.*, 19, 347, 1974.
14. A. A. Rehms and P. R. Callis, *Chem. Phys. Lett.*, 140, 83, 1987. M. R. Eftink, L. A. Selvidge, P. R. Callis, and A. A. Rehms, *J. Phys. Chem.*, 94, 3469, 1990.
15. J. W. Longworth, Excited States of Proteins and Nucleic Acids, Chapter 5, R. F. Steiner and I. Weinryb, Eds., Plenum Press, New York, 1971.
16. J. D. Westbrook and K. Krogh-Jespersen, ESPPAC (Excited States Properties PACkage), Rutgers University, 1989.
17. J. E. Ridley and M. C. Zerner, *Theor. Chim. Acta*, 32, 111, 1973. K. Krogh-Jespersen and M. A. Ratner, *J. Chem. Phys.*, 65, 1305, 1976; *Theor. Chim. Acta*, 47, 283, 1978. J. A. Pople and D. L. Beveridge, Approximate Molecular Orbital Theory, McGraw-Hill, New York, 1970.
18. D. B. Kitchen, F. Hirata, J. D. Westbrook, R. M. Levy, D. Kofke, and M. Yarmush, *J. Comput. Chem.*, 11, 1169, 1990.
19. H. J. C. Berendsen, J. P. M. Postma, W. F. van Gunsteren, and J. Hermans, Intermolecular Forces, page 31, B. Pullman, Ed., Reidel; Dordrecht, Holland, 1981.
20. R. M. Levy, M. Belhadj, and D. B. Kitchen, *J. Chem. Phys.*, 95, 3627, 1991.
21. E. Clementi, *J. Chem. Phys.*, 54, 2492, 1971.
22. E. Scrocco and J. Tomasi, *Top. Curr. Chem.*, 42, 95, 1973; *Adv. Quantum Chem.*, 11, 115, 1978.
23. R. McWeeny, *Phys. Rev.*, 126, 1028, 1962.
24. L. E. Chirlian and M. M. Francl, *J. Comp. Chem.*, 8, 894, 1987. B. H. Besler, K. M. Merz, Jr., and P. A. Kollman, *J. Comp. Chem.*, 11, 431, 1990.
25. P. O. Lowdin, *J. Chem. Phys.*, 56, 365, 1970.
26. W. J. Hehre, R. F. Stewart, and J. A. Pople, *J. Chem. Phys.*, 51, 2657, 1969.
27. The differences between the partial atomic charges shown here and those in reference 6 reflect almost exclusively the use of different point sampling schemes rather than different geometries.
28. P. Ilich, C. Haydock, and F. G. Prendergast, *Chem. Phys. Lett.*, 158, 129, 1989.
29. M. S. T. Walker, T. W. Bednar, and R. W. Lumry, *J. Chem. Phys.*, 47, 1020, 1967.
30. L. Onsager, *J. Am. Chem. Soc.*, 58, 1486, 1936.
31. V. Luzhkov and A. Warshel, *J. Am. Chem. Soc.*, 113, 4491, 1991.

Downloaded from SPIE Digital Library on 21 Oct 2009 to 128.6.69.52. Terms of Use: http://spiedl.org/terms